

# Negative refractive index in non-resonance spectrum area

Chao Xu (徐 超) and Jianfeng Dong (董建峰)\*

Institute of Optical Fiber Communication and Network Technology, Ningbo University, Ningbo 315211, China

\*E-mail: dongjianfeng@nbu.edu.cn; nbu-djf@21cn.com

Received February 25, 2010

A new concept to realize negative refractive index in non-resonance spectrum using chiral metamaterial is proposed. A low-index metamaterial is added to diminish the effective refractive index of the combined structure. Simulation and material parameter retrieval procedures are carried out to determine material performances. Results show evidence of negative refractive index and strong optical activity in the new chiral metamaterial.

OCIS codes: 160.3918, 160.1585, 160.4670.

doi: 10.3788/COL20100811.1067.

Metamaterials with negative refraction index (NRI) have attracted significant attention since their first experimental verification. This type of artificially constructed material has unique and interesting characteristics, and can provide electromagnetic properties that are difficult or impossible to be found in conventional natural materials<sup>[1–3]</sup>. Recently, theoretical and experimental studies have shown that chiral metamaterials can achieve NRI due to their chirality<sup>[4–14]</sup>. NRI chiral metamaterials can also be used as a “perfect lens” for circularly polarized waves<sup>[4,7]</sup>. Chiral medium has optical activity and shows different electromagnetic responses toward right- and left-circularly polarized (RCP and LCP) incident waves. Refractive indices for each wave are given by  $n_{\pm} = \sqrt{\mu_c \epsilon_c / \mu_o \epsilon_o} \pm \kappa$ , where  $n_+$  and  $n_-$  refer to RCP and LCP,  $\mu_c$  and  $\epsilon_c$  are the permeability and permittivity of the chiral medium, and  $\mu_o$  and  $\epsilon_o$  are the vacuum permeability and permittivity, respectively. The chirality parameter “ $\kappa$ ” has to be as large as possible to make NRI occur in one of the incident waves. However, optical activity or chirality parameter in natural chiral material is very small. Therefore, previous work has focused on fabricating artificial materials with larger chirality parameters. One way to gain a larger  $\kappa$  is through electromagnetic resonance<sup>[9–14]</sup>, because at resonance frequencies, planar or nonplanar chiral structures exhibit either electric-dipole or magnetic-dipole resonance or both. The asymmetrical nature of a chiral structure ensures that coupling between these resonances is not prohibited and is strong enough to convert polarization states. Changing polarization leads to stronger optical activity and larger chirality parameters, thus achieving negative indices in the spectrum areas.

In this letter, we propose a different concept to achieve NRI in chiral media without structure resonance. In this method, we focus on reducing the effective refractive index ( $n_{\text{eff}}$ ) of chiral media, which is equal to  $\sqrt{\mu_c \epsilon_c / \mu_o \epsilon_o}$ , making the LCP incident wave negative in non-resonance frequencies. The basic element in this study is the three-dimensional (3D) single helix, which provides the chirality parameter. Spiral structures such as DNA molecules are known to have optical activities. Previous studies have shown polarization stop bands and strong circular dichroism in such structures<sup>[15–18]</sup>. Recently, NRI has

also been achieved using spiral structures<sup>[14]</sup>. We choose spiral as the basic element because of its relatively stable electromagnetic response and moderate chirality in a considerably wide range of spectrum areas. An excessive multi-layer metal gridding is added as the second effective element to reduce  $n_{\text{eff}}$  of the structure. The array of metal wire is widely known to generate electric resonance and provide negative permittivity in certain frequency ranges. Through parameter adjustment, it could also be used as a low-index metamaterial.

Our chiral metamaterial is composed of single metal helix structures and multi-layer metal gridding. The metallic material we used in this study is gold. Figure 1 shows the structure to be simulated and analyzed. These material geometric parameters are gained through optimization. Therefore, we simulated a series of

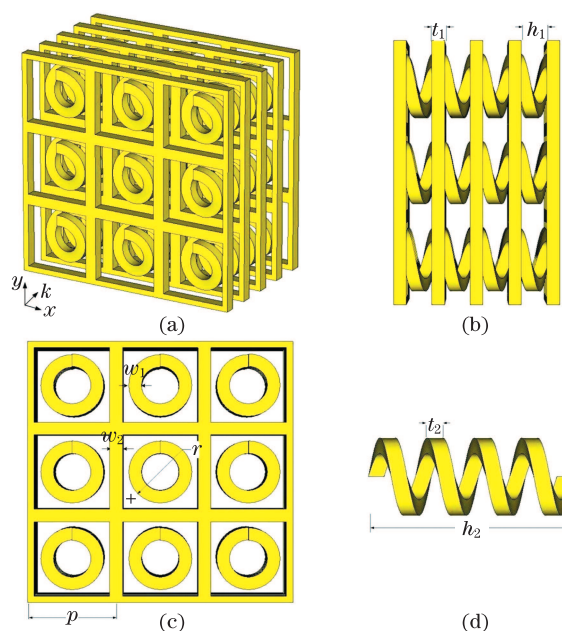


Fig. 1. Geometry of 3D chiral structure: periodic constant  $p=700$  nm, lateral height and width of spiral  $w_1 = t_2=100$  nm, total spiral height  $h_2=1200$  nm, spiral diameter  $r=250$  nm, lattice period along  $k$ -direction  $N=4$ . Height and width of metal gridding  $t_1 = w_2=100$  nm, distance between each layer  $h_1=200$  nm along  $k$ -direction.

structures with different total spiral heights  $h_2$  ranging from 800 to 2000 nm, and with different lattice periods both in-plane and longitudinal.

Numerical simulations are performed using a frequency domain finite element method. The dielectric properties of the metal gold are handled with a frequency-dependent Drude model (plasma angular frequency  $\omega_p = 2\pi \times 2081$  THz, collision frequency  $\omega_c = 2\pi \times 35$  THz). A plane wave occurs along the  $k$ -direction, normally incident onto the surface plane of the structure. The periodic boundary condition is used in the direction perpendicular to the propagation direction. Detailed calculations are used to determine the reflection and transmission coefficients from a single unit cell. The complex effective parameters  $n$ ,  $\varepsilon$ , and  $\mu$ , and the chirality parameter  $\kappa$  from the simulated transmission and reflection are obtained using the retrieval procedure for chiral metamaterial<sup>[9]</sup>.

To fully demonstrate our concept, we simulate the single helix structure, multi-layer metal gridding structure, and combined structure, and obtain their reflection and transmission coefficients. Figure 2(a) shows the calculated transmittance spectra of LCP and RCP for normal incidence along the  $k$  direction. Comparing the transmission curves of the combined structure to the former work, no obvious resonance characteristics are identified. Therefore, transmittance spectra for both polarizations are smooth. The simulated transmission phases for RCP and LCP of the combined structure are shown in Fig. 2(b). For RCP and LCP, the transmittance phases exhibit moderate phase modulations at 125- and 95-THz frequencies, respectively, in accordance with the transmittance lines in Fig. 2(a). This result again proves the non-resonance nature of the designed combined structure.

Using the retrieval procedure mentioned above, we

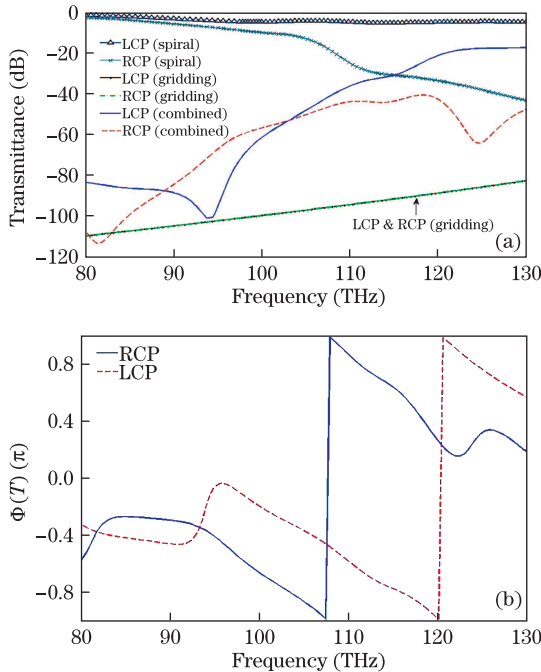


Fig. 2. (a) Simulation transmittance spectra. For the metal gridding structure, the transmission coefficients show no differences for RCP and LCP. (b) Simulation transmission phases for RCP and LCP of the combined structure.

calculate the refractive indices and chirality parameters of the combined structure and two separate components, respectively. The first column of Fig. 3 gives the numerical result of the single helix structure. The refractive indices for LCP and RCP are obviously different due to chirality. However, for the single helix structure, none of the two incident polarizations is negative because its effective refractive index  $n_{\text{eff}}$  is significantly larger than the real part of its chirality parameter. The second column of Fig. 3 shows the refractive indices and chirality parameter of the multi-layer metal gridding structure. The value of  $\kappa$  is constantly zero throughout the whole spectra because of the symmetric nature of the gridding structure (Fig. 3(d)). No differences are seen between LCP and RCP propagation in the metal gridding; thus, their refractive indices both equal  $n_{\text{eff}}$ . Moreover,  $n_{\text{eff}}$  in the spectrum area below 120 THz (Fig. 3(d)) is significantly flattened and has an approximate value of 0.2, which nearly approaches zero compared with the  $n_{\text{eff}}$  curve of the spiral structure (Fig. 3(a)). Therefore, we can refer it as a low-index metamaterial.

However, the multi-layer gridding structure used here is different from the fishnet structure studied as an alternative method to achieve NRI via a different mechanism<sup>[19,20]</sup>. The fishnet structure is often regarded as a holey plasmonic metamaterial<sup>[21]</sup> because the ratio between hole size and lateral feature size is well below 3. In comparison, in this study, the ratio between hole-width and line-width of the metal gridding is 6 in both the  $x$  and  $y$  directions, making the structure more mesh-like. Functional wavelength is also much larger compared with the in-plane and longitudinal lattice periods  $p$  and  $h_1$ . Thus, the holey and Fabry-Perot resonances become very weak along the longitudinal direction. This is proven in Fig. 2(a), where no resonance peaks appear in the transmittance spectra of the multi-layer gridding structure.

Based on the previous discussion, none of the two components is negative index metamaterial. However, when we combine the two structures by filling the hole of the metal gridding with a single helix, the electromagnetic response of the combined structure becomes completely different (Fig. 2(a)). There are strong electromagnetic couplings between spirals and their adjacent metal griddings. Moreover, the area of metal becomes significantly larger in the direction perpendicular to the  $k$  direction. These two reasons lead to the fact that  $n_{\text{eff}}$  of the combined structure is quite small (even below zero around 95 THz) compared with the single helix structure. However, the absolute value of  $\kappa$  of the combined structure is almost the same as the single helix. Consequently, LCP becomes negative in a considerable wide band range, whereas RCP remains positive (Figs. 3(h) and (i)).

Finally, we calculate the material and optical parameters to demonstrate that the negative index in this medium is due to chirality (Fig. 4). In Fig. 4(b), permeability  $\mu$  is constantly positive throughout the spectra, while in Fig. 4(a), permittivity  $\varepsilon$  is negative below 108 THz. Thus, no frequency band exists when  $\mu$  and  $\varepsilon$  become simultaneously minus, showing evidence that NRI in this material is due to chirality. Moreover, no electric or magnetic resonances occur around the spectrum area where the refractive index becomes negative.

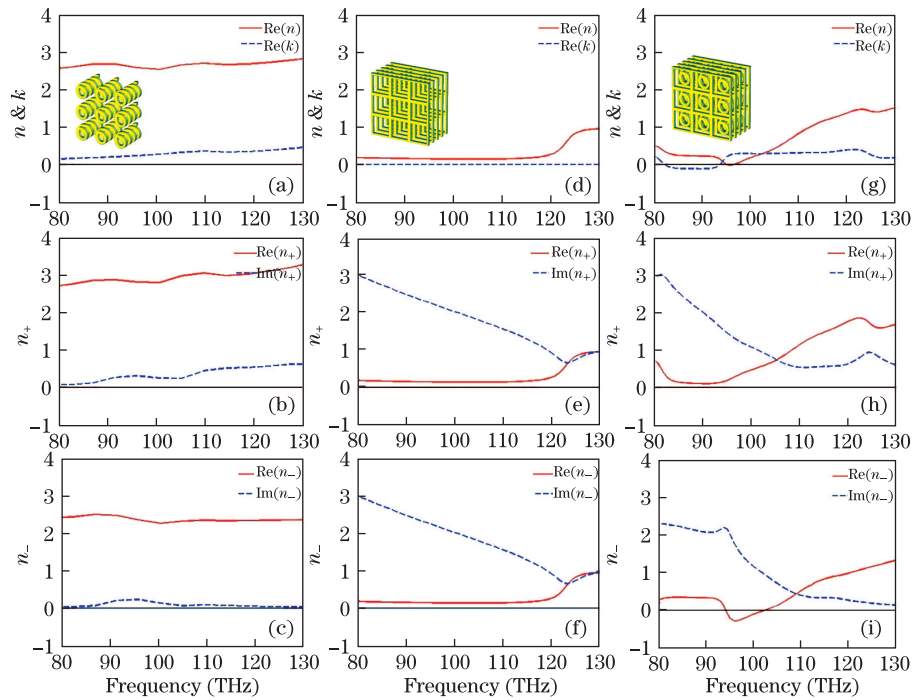


Fig. 3. Refractive indices and chirality parameters. (a)–(c) Single helix structure; (d)–(f) multi-layer metal gridding; (g)–(i) Combined structure.

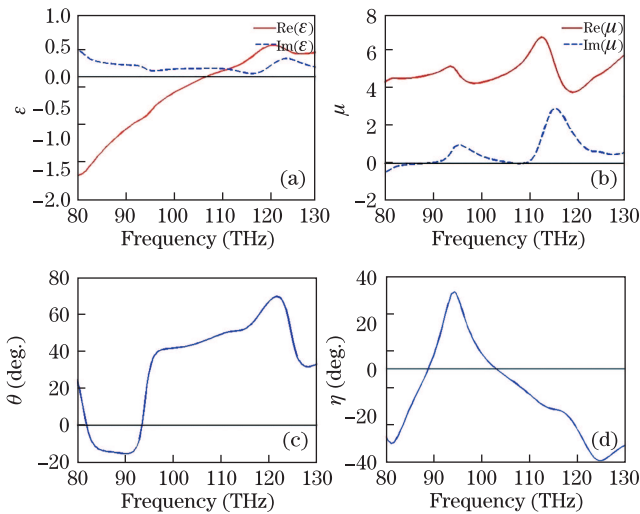


Fig. 4. Material and optical parameters of the combined chiral structure. (a) Permittivity  $\epsilon$ ; (b) permeability  $\mu$ ; (c) Polarization azimuth rotation  $\theta$ ; (d) ellipticity angle  $\eta$ .

This property of material parameter curves is in accordance with the property of transmission curves we have previously discussed, and again proves that the NRI outcome is attributed to the diminishing effective index of the structure.

Optical activity is well known to be a major characteristic of chiral metamaterials. In Figs. 4(c) and (d), we present the optical performance of our structure by demonstrating its polarization azimuth rotation angle  $\theta$  and ellipticity angle  $\eta$ . The new combined chiral medium shows clear and strong optical activities, and its polarization azimuth rotation angle is comparably stable in most spectra, up to  $70^\circ$  at its maximum. This figure is significantly larger than the value gained using gammadion

structures<sup>[22,23]</sup>. At the frequency range between 100 and 110 THz, we also gain a polarization rotation exceeding  $40^\circ$  with  $\eta=0$ , which is about four times larger than the value reported in bilayer chiral metamaterials<sup>[10,24]</sup>.

In conclusion, the double-element chiral metamaterial we proposed shows strong optical activity in the simulated frequency range. Calculation of material parameters and comparison of refractive indices of two separate element structures reveal the chiral nature of the combined structure. Together with the retrieved refractive parameters of the combination, a new metamaterial with NRI due to chirality is shown. In addition, achieving NRI in a non-resonance spectrum area via adding a low-index metamaterial in a conventional chiral structure provides an alternative concept in metamaterial design.

This work was supported by the National Basic Research Program of China (No. 2004CB719805), the National Natural Science Foundation of China (No. 60777037), the Natural Science Foundation of Zhejiang Province (No. Y1091139), and the K. C. Wong Magna Fund in Ningbo University.

## References

1. S. Wen, X. Dai, and Y. Xiang, Chinese J. Lasers (in Chinese) **35**, 803 (2008).
2. Z. Wang, J. Zhou, L. Zhang, H. Ren, and C. Jin, Acta Opt. Sin. (in Chinese) **28**, 1558 (2008).
3. D. Cao, H. Zhang, and F. Tao, Acta Opt. Sin. (in Chinese) **28**, 1601 (2008).
4. C. Monzon and D. W. Forester, Phys. Rev. Lett. **95**, 123904 (2005).
5. J. B. Pendry, Science **306**, 1353 (2004).
6. S. Tretyakov, A. Sihvola, and L. Jylhä, Photon. Nanostruct. Fundam. Appl. **3**, 107 (2005).

7. Y. Jin and S. He, *Opt. Express* **13**, 4974 (2005).
8. D.-H. Kwon, D. H. Werner, A. V. Kildishev, and V. M. Shalaev, *Opt. Express* **16**, 11822 (2008).
9. E. Plum, J. Zhou, J. Dong, V. A. Fedotov, T. Koschny, C. M. Soukoulis, and N. I. Zheludev, *Phys. Rev. B* **79**, 035407 (2009).
10. S. Zhang, Y.-S. Park, J. Li, X. Lu, W. Zhang, and X. Zhang, *Phys. Rev. Lett.* **102**, 023901 (2009).
11. J. Zhou, J. Dong, B. Wang, T. Koschny, M. Kafesaki, and C. M. Soukoulis, *Phys. Rev. B* **79**, 121104 (R) (2009).
12. B. Wang, J. Zhou, T. Koschny, and C. M. Soukoulis, *Appl. Phys. Lett.* **94**, 151112 (2009).
13. J. Dong, J. Zhou, T. Koschny, and C. Soukoulis, *Opt. Express* **17**, 14172 (2009).
14. M. C. K. Wiltshire, J. B. Pendry, and J. V. Hajnal, *J. Phys.: Condens. Matter* **21**, 292201 (2009).
15. M. Thiel, M. Decker, M. Deubel, M. Wegener, S. Linden, and G. von Freymann, *Adv. Mater.* **19**, 207 (2007).
16. P. C. P. Hrudey, B. Szeto, and M. J. Brett, *Appl. Phys. Lett.* **88**, 251106 (2006).
17. M. Mitov and N. Desso, *Nature Mater.* **5**, 361 (2006).
18. M. Thiel, G. von Freymann, and M. Wegener, *Opt. Lett.* **32**, 2547 (2007).
19. G. Dolling, M. Wegener, and S. Linden, *Opt. Lett.* **32**, 551 (2007).
20. J. Valentine, S. Zhang, T. Zentgraf, E. Ulin-Avila, D. A. Genov, G. Bartal, and X. Zhang, *Nature* **455**, 376 (2008).
21. A. Mary, S. G. Rodrigo, F. J. Garcia-Vidal, and L. Martin-Moreno, *Phys. Rev. Lett.* **101**, 103902 (2008).
22. M. Kuwata-Gonokami, N. Saito, Y. Ino, M. Kauranen, K. Jefimovs, T. Vallius, J. Turunen, and Y. Svirko, *Phys. Rev. Lett.* **95**, 227401 (2005).
23. K. Konishi, B. Bai, X. Meng, P. Karvinen, J. Turunen, Y. P. Svirko, and M. Kuwata-Gonokami, *Opt. Express* **16**, 7189 (2008).
24. A. V. Rogacheva, V. A. Fedotov, A. S. Schwanecke, and N. I. Zheludev, *Phys. Rev. Lett.* **97**, 177401 (2006).